NH$_2$ detection in fuel-nitrogen combustion using an Alexandrite laser

C. Brackmann[*], B. Zhou, Z.S. Li, M. Aldén

Combustion Physics, Lund University, Box 118, SE-221 00 Lund, Sweden

Abstract

A scheme for NH$_2$ detection by means of laser-induced fluorescence (LIF) with excitation in the ultraviolet-blue regime around 385 nm, in particular using the second harmonic of a solid-state Alexandrite laser, is presented. This alternative provides interference-free detection with improved signal compared with previously employed concepts based on Nd:YAG and dye-laser excitation in the visible regime. A detection limit in the range 500-1000 ppm was estimated for planar single-shot LIF imaging on centimeter-scale.

Introduction

With a large part of energy-production world-wide based on combustion and increased attention to limited resources of fossil fuels, interest in renewable, biomass-derived, nitrogen-containing fuels has increased. This makes improved understanding of fuel-nitrogen combustion chemistry highly relevant and insights in these processes for development and verification of kinetic mechanisms require accurate experimental data on the combustion process.

Figure 1 shows a simplified schematic layout of the combustion chemistry of a fuel containing hydrocarbon and nitrogen components. The hydrocarbon and nitrogen chemistries are presented in the left and right parts of Fig. 1, respectively. The fuel-nitrogen chemistry contains two paths, involving oxidation of hydrogen cyanide (HCN) and ammonia (NH$_3$) [1]. The amidogen (NH$_2$) radical is a key species in the ammonia oxidation path as shown in the right part of Fig. 1. In addition it is an important component in the thermal De-NO$_x$ process [1, 2]. Thus, experimental data on NH$_2$ are very valuable for understanding fuel-nitrogen combustion.

Laser-based techniques provide powerful non-intrusive methods with high temporal and spatial resolution for characterization of combustion [3]. Laser-induced fluorescence (LIF) provides specific detection with high sensitivity for many combustion-relevant species. In addition, the technique allows for planar and in some cases also volumetric imaging. Related to fuel-nitrogen chemistry, laser-based methods have been readily developed and applied for detection of diatomic nitrogen radicals such as NH [4] and CN [5]. Investigations have also been carried out monitoring more complex molecules containing three or more atoms such as HCN [6], NH$_2$ [4, 7-12] and NH$_3$ [13].

Measurements of NH$_2$ in flames have been made using absorption spectroscopy, for example in ammonia-oxygen flames at low as well as atmospheric pressure [7, 8]. In addition, sensitive intracavity absorption spectroscopy has been employed for NH$_2$ detection in NH$_3$-doped CH$_4$-air flames [11].
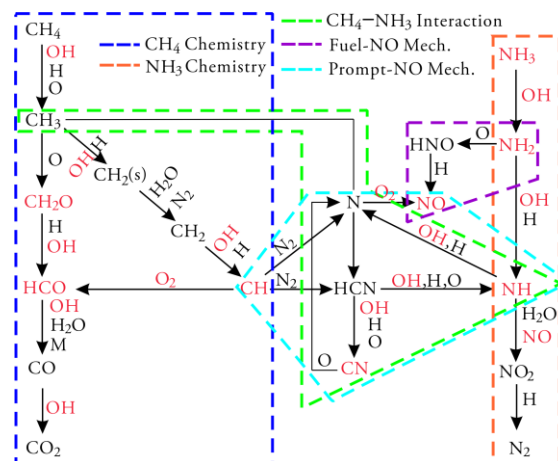

Figure 1. Schematic layout of the chemistry for combustion of a fuel containing hydrocarbon and nitrogen components represented by oxidation pathways of CH$_4$ (left) and HCN/NH$_3$ (right). The NH$_2$ radical is a key species in the NH$_3$ pathway (upper right).

The NH$_2$ radical has a wide absorption spectrum covering the range 390-800 nm for transitions in the $\tilde{A}^2A_1 \leftarrow X^2B_1$ system [14]. The NH$_2$ ground state is bent whereas the excited state is a close to linear configuration and the spectrum consists of multiple bands of the bending vibrational mode. Rotational transitions are assigned by three quantum numbers N, K$_a$, and K$_c$ written in notation N$_{KaKc}$. Further details on NH$_2$ spectroscopy and spectroscopic notation are given in ref. [14]. The absorption studies cited above were made at wavelengths around 600 nm probing the (0,9,0) vibrational band. Excitation in this wavelength regime has also been employed for LIF measurements of NH$_2$ in nitrogen-doped hydrocarbon flames at low pressure [4, 12] as well as NH$_3$ flames at atmospheric pressure [10]. In addition NH$_2$ LIF measurements in atmospheric pressure flames have been made using a krypton ion laser at 647 nm [9].

This work presents an alternative approach for NH$_2$ detection by means of LIF with excitation in the ultraviolet-blue regime around 385 nm. In particular this

---

can be achieved by the second harmonic of a powerful solid-state Alexandrite laser. This laser has proven to be advantageous for detection of radicals CH [15] and HCO [16] due to its longer pulse duration compared with Nd:YAG dye laser systems often used for combustion diagnostics. The NH_2 excitation scheme is characterized in terms of spectroscopy and chemical selectivity in flame as well as a NH_2 gas flow generated by laser-induced photolysis of NH_3. The NH_2 signal strength is compared with previously employed LIF excitation in the visible regime, the potential influence of photochemical effect is addressed, and the potential for planar LIF imaging of NH_2 is investigated.

Experimental

Measurements were made in an ammonia-air flame stabilized on a special porous-plug burner (Holthuis & Associates), consisting of a 60 mm porous bronze plug with a 2 mm diameter central hole. A central conical jet flame was stabilized above the hole and a one-dimensional, flat co-flow pilot flame was stabilized on the surrounding plug. Mixtures of NH_3-air and CH_4-air were independently fed into the central jet and the surrounding co-flow, respectively. The co-flow pilot flame was operated at stoichiometry while an NH_3-air flame of equivalence ratio $\Phi=1.4$ was stabilized on the jet. The jet flows of NH_3 and air were 0.26 l/min and 0.69 l/min, respectively whereas the pilot flame was supplied with 1.2 l/min of CH_4 and 11.2 l/min of air. All flows were set by mass-flow controllers (Bronkhorst).

Fluorescence experiments on NH_2 were carried out using two laser systems. A combined Nd:YAG (Quanta-Ray PRO 250-10, Spectra Physics) and dye laser (Cobra Stretch-G-2400, Sirah) system operating at 10 Hz repetition rate and with 8 ns pulse duration. The dye laser was operated using Rhodamine 610 generating a tunable beam in the wavelength range 600-635 nm. The red beam was combined with the 1064 nm fundamental of the Nd:YAG laser in a frequency-mixing crystal to generate wavelengths in the range 385-390 nm. The maximum output pulse energy achieved with this arrangement was 15 mJ. These wavelengths were also accessed by the second harmonic of a linear cavity Alexandrite laser (101-PAL, Light Age Inc.). The Alexandrite laser repetition rate was 10 Hz, the pulse duration typically 70 ns, the laser linewidth around 2.5 cm^{-1}, and the maximum output pulse energy about 70 mJ. For comparison with previous work on NH_2 detection by LIF [10], excitation was also carried out in the visible regime at 630 nm using the dye laser output beam without mixing.

The NH_2 data were also supplemented by measurements of NH_3 and NH fluorescence profiles. Two-photon excitation of NH_3 was induced in the C'-X (2-0) band while NH was probed in the $A^3\Pi-X^3\Sigma^-$ (1-0) band, both located at wavelengths around 305 nm and accessed by frequency-doubling the dye laser.

In addition to detection in flame, NH_2 was also generated by means of ultraviolet laser photolysis of NH_3 mixed with Argon in a gas flow at room temperature. The 213 nm fifth harmonic of a Nd:YAG laser (Brilliant B, Quantel) was used for photodissociation of NH_3 with a pulse energy of 6 mJ.

In most investigations the laser beams were focused into small sheets using an f=+200 mm cylindrical lens. However, the NH_2 excitation at 630 nm required focusing with a spherical lens of f=+200 mm in order to achieve appreciable signal. For direct comparison a set of measurements were also made with the 385 nm Alexandrite laser beam focused by the spherical lens. For imaging the Alexandrite laser beam was shaped into a focused sheet, ~20 mm high, using a cylindrical lens of f=-40 mm combined with an f=+200 mm spherical lens.

The signals were detected with intensified CCD cameras (Princeton Instruments, PI-MAX I/II). For NH_2 measurements an f=50 mm objective (Nikkor f/1.2) was mounted on the camera whereas an f=50 mm UV lens (Universe f/3.5) was used for detection of NH and NH_3. Extension tubes were used to obtain suitable image magnification. Longpass filters GG400 and RG630 (Schott AG) were used to suppress the laser excitation wavelength for excitation of NH_2 at 385 and 630 nm, respectively. The GG400 filter was also used for detection of NH_3 fluorescence.

Results & Discussion

Figure 2a shows a fluorescence excitation spectrum measured in the Φ=1.4 NH$_3$-air flame when scanning the dye laser from 385 to 390 nm. A complex spectrum containing a dense overlapped line structure can be observed.
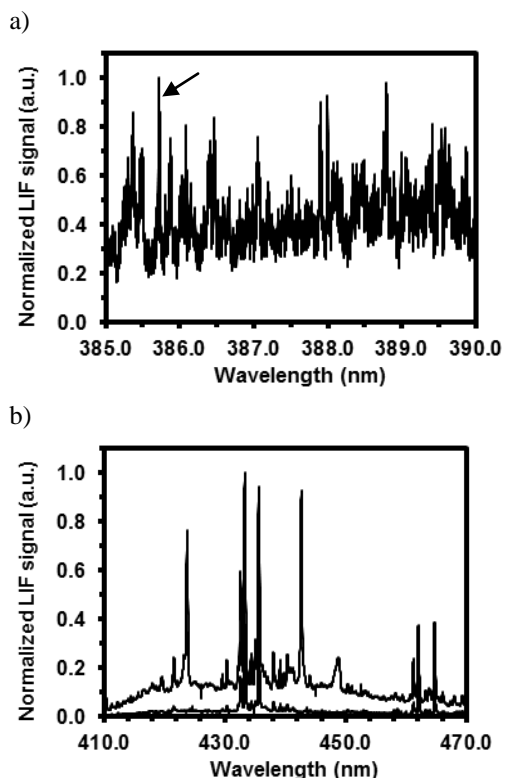
a)

b)

Figure 2. a) Excitation scan fluorescence spectrum measured in Φ=1.4 NH$_3$-air flame. A dense spectrum attirbuted to NH$_2$ can be observed. b) Fluorescence emission spectra obtained for excitation at 385.7 nm (arrow in (a)) with Nd:YAG dye laser and Alexandrite laser. NH$_2$ fluorescene bands around 430 and 460 nm can be identified. The stronger spectrum from Alexandrite excitation also shows Raman lines from N$_2$ (~424 nm) and NH$_3$ (~445 nm).

A rather narrow and distinct spectral line is seen at 385.7 nm and fluorescence emission spectra detected with the dye laser and the Alexandrite laser positioned at this line are shown in Fig. 2b. Both spectra show fluorescence emission lines in wavelength ranges 430-440 nm and 460-470 nm, corresponding to the locations of the (0,15,0) and (0,14,0) vibrational bands reported for NH$_2$ [14]. In addition, the spectrum acquired using the more powerful Alexandrite laser also shows Raman lines from N$_2$ and fuel NH$_3$ at wavelengths 424 and 445 nm, respectively.

Even though the structures identified in the flame spectra suggest NH$_2$, investigations were also made in a room-temperature NH$_3$-argon jet from which NH$_2$ was created by means of laser photolysis. This enables investigations in a less complicated chemical environment at lower temperature. An excitation scan spectrum measured in the NH$_3$-argon jet is shown in Fig. 3a. Compared with the flame spectrum the line structure is less complicated and can be assigned to NH$_2$ by comparison with spectroscopic data from literature [17]. The scanned spectra contain transitions of the (0,19,0) vibrational band and in particular the spectral line at 385.7 nm can be identified as mainly consisting of the two spin components the 3_{03} $\tilde{A}(0,19,0)\Sigma \leftarrow 4_{13}$ X(0,0,0) transition.

Figure 3b shows fluorescence emission spectrum measured in the NH$_3$-argon jet. In agreement with flame data, fluorescence bands can be observed around 430 and 460 nm. In addition the spectrum of the NH$_3$-argon jet also includes a peak at 336 nm, corresponding to NH (0-0) A$^3\Pi$-X$^3\Sigma^-$ transitions, as well as a strong peak of at 385 nm corresponding to elastically scattered laser radiation. Thus, it can be concluded that the fluorescence signal obtained in the NH$_3$-air flames for excitation in the 385-390 nm region is generated by NH$_2$.
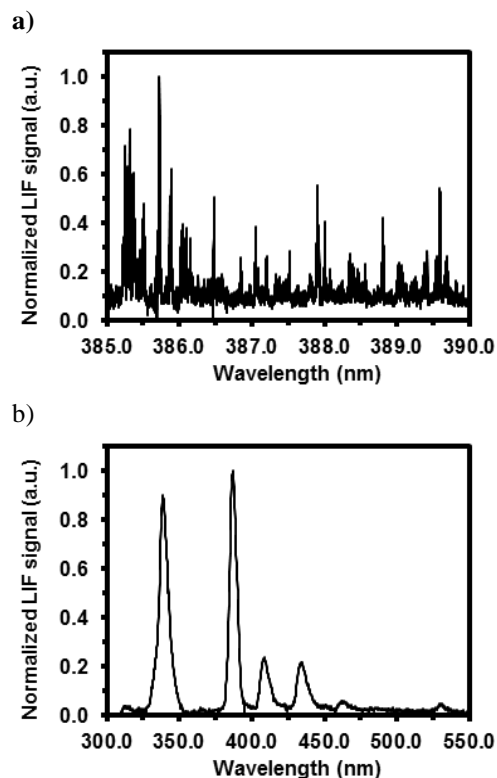
a)

b)

Figure 3. a) Excitation scan fluorescence spectrum measured in a room-temperature NH$_3$-argon jet after NH$_3$ photolysis. Spectral lines of NH$_2$ can be identified and correspond to peaks identified in the flem spectrum. b) Fluorescence emission spectrum obtained for excitation at the peak indicated in (a), 385.7 nm. A peak of elastically scattered laser ligh is observed at 385 nm together with fluorscence bands from NH (~336 nm) and NH$_2$ (~430 and ~460 nm).

Flame diagnostics of NH$_2$ by means of laser-induced fluorescence has previously been carried out using excitation in the visible regime, for example by Copeland et al. [10]. For direct comparison, NH$_2$

3

excitation was also carried out using 630 nm probing the (0,8,0) band and resulting in the dotted NH$_2$ profile presented in Fig. 4a.
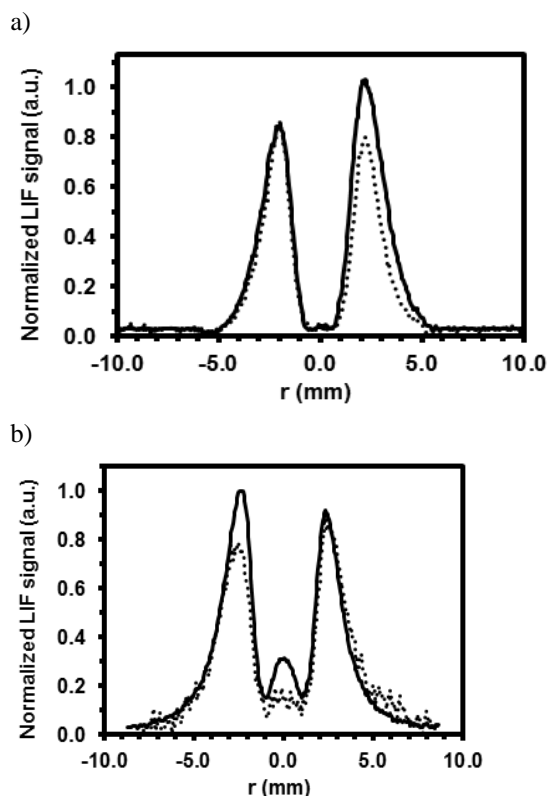
a)

b)

Figure 4. NH$_2$ profiles measured in Φ=1.4 NH$_3$-air flame. a) Alexandrite laser excitation at 385.7 nm (solid) and dye laser excitation at 630 nm (dotted) in the NH$_2$ (0,8,0) band, similar to the approach of Copeland et al. [10] b) Normalized NH$_2$ profiles measured using Alexandrite laser excitation of irradiances of 170 (solid) and 10 MW/cm^2. The similar shape of the NH$_2$ peaks on each side of the flame indicate no observable photochemical effects on the detected signal.

The dotted NH$_2$ profile shows very good agreement in shape with that of a profile measured using the Alexandrite laser tuned to 385.7 nm, also shown in Fig. 4a. This agreement further confirms the detection of NH$_2$ in the flame. However, the dotted profile has been multiplied by a factor of 10 to make it comparable in strength to the solid one. For a comparison of signal strengths the detection efficiency needs to be considered and the CCD detector sensitivity is typically a factor of 3 lower at red wavelengths compared with blue. This suggests that excitation in the blue regime using the spectrally broad Alexandrite laser provides at least three times stronger NH$_2$ signal compared with excitation at longer wavelengths.

Excitation at shorter wavelengths increases the risk for undesirable photo-induced chemistry, which needs to be considered. Figure 4b presents two NH$_2$ profiles measured at laser irradiances 170 and 10 MW/cm^2, corresponding to pulse energies of 70 and 4 mJ,

respectively. The profiles have been normalized and show similar NH$_2$ distributions even though an extra contribution from the NH$_3$ fuel can be seen at position 0 mm in the center for the profile acquired at high irradiance. Nevertheless, the similarity in NH$_2$ distributions indicates that potential photochemical effects do have observable impact on the NH$_2$ signal.
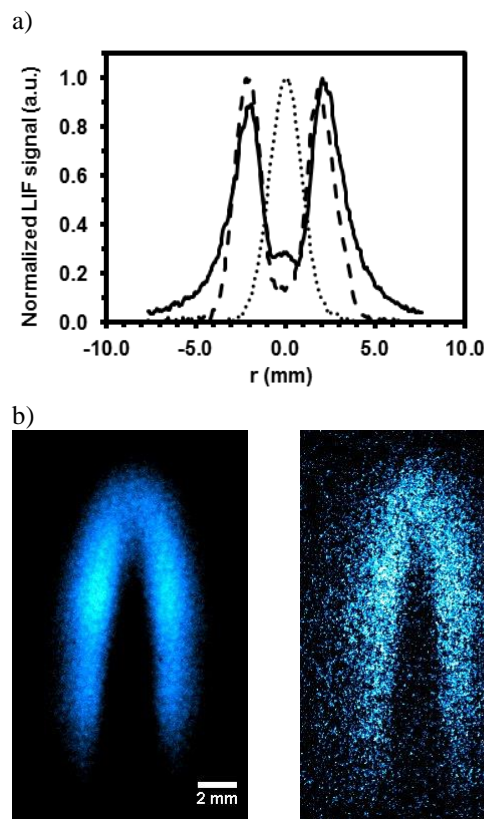
a)

b)

Figure 5. Radial profiles of NH$_2$ (solid), NH (dashed), and NH$_3$ (dotted) measured in Φ=1.4 NH$_3$-air flame. Both radicals shows partial overlap with the NH$_3$ fuel and corresponding gradients towards the reactant side. b) NH$_2$ fluorescence images, 300-shot average (left) and singe-shot (right) with signal-to-noise ratio ~ 3.

Figure 5 presents further results from NH$_2$ diagnostics in the Φ=1.4 NH$_3$-air flame. A normalized NH$_2$ fluorescence profile is shown in Fig. 5a together with normalized profiles of NH and NH$_3$ measured in the same flame. The NH$_3$ fuel profile consists of a single peak centered on the middle of the burner while the radical profiles show symmetric shapes with two peaks each located on the sides. In agreement with simulations and experimental results for one-dimensional NH$_3$-air flames the fuel and nitrogen-radical profiles show partial overlap into the reaction zone. On the reactant side towards the inner of the flame cone the radical species show rather steep gradients, which can be considered to overlap as observed differences are within the uncertainty in measurement position. On the outer side of the flame cone NH$_2$ extends longer into the product zone than the NH. The observed profile shape is in agreement with those of NH$_2$ fluorescence profiles

measured in a $H_2/N_2O/N_2$ flame by Wong et al. [9]. In addition the experimental data shows similar trends as NH_2 and NH profiles obtained from a CHEMKIN simulation of a one-dimensional NH_3-air flame of the same stoichiometry (data not shown).

Figure 5b shows examples of NH_2 LIF imaging for excitation at 385.7 nm in the $\Phi=1.4$ NH_3-air flame. The images were acquired using a 20 mm high laser sheet covering the flame tip region. The NH_2 distribution is clearly visualized in the left image which is an average over 100 laser pulses. A ~2 mm wide NH_2 layer can be observed in the flame tip region. Non-stationary conditions require single-shot imaging as exemplified in the right image in which the NH_2 region also is visualized. With the detection noise represented by the standard deviation in an image region absent of fluorescence signal the single-shot image signal-to-noise ratio is 3. Simulations of a one-dimensional $\Phi=1.4$ NH_3-air flame show a peak NH_2 mole fraction around 1000 ppm and absorption measurements of NH_2 in fuel-rich NH_3-O_2 flames by Chou et al. resulted in peak NH_2 molar fractions around 800 ppm [8]. Assuming similar NH_2 concentration for the flame imaged in Fig. 5b suggests a detection limit for single-shot imaging in the range 500-1000 ppm. For measurements using a laser beam focused along a line data indicate a signal increase by a factor of 3-4, resulting in a detection limit of a few hundred ppm.

Conclusion

Laser-induced fluorescence detection of NH_2 in combustion has been characterized for excitation of the $(0,9,0)$ $\tilde{A}^2A_1 \leftarrow (0,0,0)$ X^2B_1 at 385.7 nm. Utilization of the second harmonic of an Alexandrite laser for this purpose provides improved NH_2 probing with interference-free detection. In addition, the scheme allows for fluorescence imaging up to centimeter scale for NH_2 concentrations approaching 1000 ppm. Altogether the presented approach provides enhanced possibilities for characterization of fuel-nitrogen combustion chemistry.

References

1. J. A. Miller; C. T. Bowman, Prog Energ Combust 15 (4) (1989) 287-338
2. R. K. Lyon, Environ Sci Technol 21 (3) (1987) 231-236
3. K. Kohse-Höinghaus; J. B. Jeffries (Ed.)^(Eds.), Applied Combustion Diagnostics, Taylor&Francis, New York, 2002.
4. B. A. Williams; J. W. Fleming, Combust Flame 110 (1-2) (1997) 1-13
5. B. Zhou; C. Brackmann; Z. S. Li; M. Aldén, Combust Flame (2014)
6. Z. W. Sun; Z. S. Li; A. A. Konnov; M. Aldén, Combust Flame 158 (10) (2011) 1898-1904
7. R. M. Green; J. A. Miller, J Quant Spectrosc Ra 26 (4) (1981) 313-327
8. M. S. Chou; A. M. Dean; D. Stern, J Chem Phys 76 (11) (1982) 5334-5340
9. K. N. Wong; W. R. Anderson; J. A. Vanderhoff; A. J. Kotlar, J Chem Phys 86 (1) (1987) 93-101
10. R. A. Copeland; M. L. Wise; K. J. Rensberger; D. R. Crosley, Appl Optics 28 (15) (1989) 3199-3205
11. I. Rahinov; A. Goldman; S. Cheskis, Combust Flame 145 (1-2) (2006) 105-116
12. M. C. Branch; M. E. Sadeqi; A. A. Alfarayedhi; P. J. Vantiggelen, Combust Flame 83 (3-4) (1991) 228-239
13. C. Brackmann; O. Hole; B. Zhou; Z. S. S. Li; M. Aldén, Appl Phys B-Lasers O 115 (1) (2014) 25-33
14. K. Dressler; D. A. Ramsay, Philos Tr R Soc S-A 251 (1002) (1959) 553-&
15. Z. S. Li; J. Kiefer; J. Zetterberg; M. Linvin; A. Leipertz; X. S. Bai; M. Aldén, P Combust Inst 31 (2007) 727-735
16. B. Zhou; J. Kiefer; J. Zetterberg; Z. S. Li; M. Aldén, Combust Flame 161 (6) (2014) 1566-1574
17. J. Xin; H. Y. Fan; I. Ionescu; C. Annesley; S. A. Reid, J Mol Spectrosc 219 (1) (2003) 37-44